EasyChair Preprint

№ 8894

Developing a Full-Body Finite Element Model and Its Validation for Seating Comfort

Shenghui Liu, Philippe Beillas, Ding Li and Xuguang Wang

October 3, 2022

Developing a Full Body Finite Element Model and Its Preliminary Validation for Seating Comfort

Abstract

Human body finite element (FE) models can be used for seating comfort assessment by providing biomechanical related parameters such as internal loads and soft-tissue deformations. However, most of the published models were only validated under a simplified condition which was usually far from a real seating situation or only adopted one posture using a single, specific seat. Their ability to be repositioned may also be limited. In recent years, an open-source PIPER software package has been developed to help personalize and position Human Body Models (HBMs) for crash simulation. Recently, we have morphed the PIPER Child model into an adult FE model. In this paper, we presented how the initially morphed adult FE model was adapted for assessing seating comfort and validated for different postures. A reconfigurable experimental seat and pressure mats were employed for its validation. Four seat configurations were defined with the seat pan angle (SPA) from 0° to 15° (5° in steps) and seat pan to seat backrest angle (SP2BA) kept to 100°. According to the preliminary results, the body seat contact area (ContactA), peak pressure (PeakP), mean pressure (MeanP), and pressure profiles (summation of pressure in columns (SOC) and summation in rows (SOR) showed good agreement with experimental observations. The full-body FE model developed and validated in this work will be used as a reference for further development of scalable and positionable models using the PIPER software framework. The model will be open source to facilitate reuse and further improvements.

Keywords: Seating dis/comfort, Full-body finite element model, Open-source, Validation

Introduction

People spend more and more time in a seating posture for transportation, office work, or leisure (Le and Marras 2016). Improving seating comfort is not only a sale argument for seat manufacturers (Grujicic et al., 2009) but also important for consumers and healthcare-related fields (Oomens et al., 2015). Sustained loads on the soft tissue of the buttocks may cause seating discomfort or even physiological problems (Elsner & Gefen, 2008), especially for drivers and wheel-chair users (Cheng et al., 2018). However, soft tissue deformations and internal loading in terms of strain, and stress, which are generally considered relevant for seating discomfort assessment, cannot be all directly measured in vivo (De Looze et al., 2003).

With the development of computational capability, more and more research has been devoted to build Finite Element (FE) HBM to analyze the causes of seating discomfort (Du et al., 2013; Levy et al., 2014).

However, most of these models were not validated under real seating conditions including several postures, therefore limiting their application to real world. For example, Al-Dirini et al. (2016) validated the model using only a rigid seat pan without a soft cushion. Huang et al. (2015) and Du et al. (2013) validated their models with a real seat under only one seat configuration. However, more seating conditions are needed for validating their sensitivity to seat parameter changes for seat comfort assessment.

In recent years, an open-source software package has been developed to personalize and position HBMs for crash simulation (available at www.PIPER-project.org). We also recently described the ongoing development of a full body adult FE model, morphed from the PIPER Child model (Liu et al., 2020). In this paper, we present how the initially morphed model was further adapted for assessing seating comfort at first, and then the preliminary validation results using the experimental data collected from a reconfigurable seat.

Model development

Developing a full-body finite element model is a time-consuming and complex process. Therefore, an open-source model, the PIPER Child model for impact simulation, was morphed into an adult-sized model. The baseline child model corresponds to a 6 years old child, 1146 mm in stature. It includes 353 parts (deformable skull, brain, abdomen muscles, internal organs, neck, neck muscles, and pelvis, etc.) for a total of 531000 elements. The model has been validated under multiple conditions for traffic injury assessment such as side-impact, and regional part validation including head, femur, neck, etc.(Beillas et al., 2016).

Brief description of the initial morphing

As presented in (Liu et al., 2020), we have morphed the PIPER child model into an adult male. The morphing target was a male aged 40 years, 1740 mm in stature and 77.6 kg in weight. The morphing was based on different types of data collected on the same person. The spine and pelvis were positioned using their 3D reconstructions from a MRI study corresponding to a seated position with seat pan to backrest angle of 100° (Beillas et al., 2009). The same seating condition was reproduced for scanning the external body shape with a handheld laser scanner. After building the geometrical targets, the model was morphed by kriging interpolation using the PIPER software. The geometric errors and the elements quality were checked, and the model was used as the basis for further work.

Model adaptation

Numerous changes were carried out on the morphed model to adapt it to the comfort application. The main objectives were to (1) symmetrize it (2) reduce its computational cost (2) refine the mesh in regions of

interest for comfort (3) adapt its material properties, which were initially selected for high-speed impact, for comfort applications.

The work was initiated by symmetrizing the model with respect to the sagittal plane. The PIPER child model geometry and mesh are mostly symmetric. The exceptions are (1) the internal organs, which are not expected to be symmetric and will not be symmetrized, and (2) the mesh of some vertebrae and of the sternoclavicular ligaments, which will be symmetrized. Furthermore, the target geometry was directly derived from experimental data and hence, the geometry of the morphed model is not symmetric.

The vertebral meshes from the 12th thoracic vertebra (T12) to the 5th lumbar vertebra (L5) were first symmetrized within the PIPER child model (including intervertebral discs). For this, one side of the vertebral mesh was kept. This half side was used to generate solid elements before symmetrizing it (Figure 1 a and b). The sternoclavicular ligaments were also symmetrized by keeping one of the two sides.

The mesh symmetry of the child model and the fact that the morphed model uses the same numbering scheme were then exploited to symmetrize the morphed model. First, the pairs of nodes that are symmetric with respect to the midsagittal plane and nodes laying on the midsagittal plane were identified in the child model. This allowed computing symmetric positions of these nodes on the morphed model by averaging (e.g. skeletal symmetry). However, this cannot be directly applied to the model as this approach would not transform the non-symmetric structures (e.g. internal organs). Hence, the symmetrized nodes were used as control points to transform the model using the Kriging in PIPER.

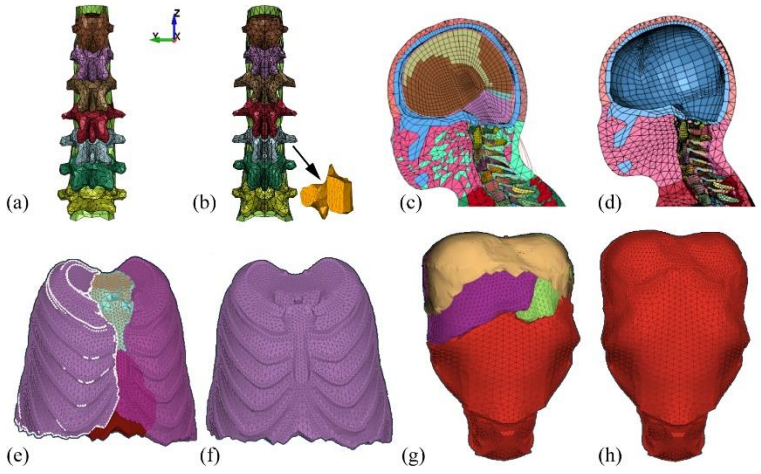

Figure 1 (a) Asymmetric lumbar vertebrae and intervertebral disc (b) Lumbar symmetrized vertebrae (c,d) Brain and neck muscles simplifications (e,f) Chest simplification (g,h) Abodomen simplification

The computational cost was then addressed. Some anatomical components which are marginally relevant for seating comfort were deleted, including the brain (initially modeled using hexahedral elements) and

neck muscles (Figure 1 c and d). The mass of the brain was compensated for by increasing the skull density. The internal organs were also simplified into two incompressible controlled volumes described by their envelope (similar to airbags): one for the chest (Figure 1 e and f), and one for the abdomen organs (Figure 1 g and h). The mass of the organs was evenly distributed onto the nodes of the envelopes. When deformable, the properties of the bones were changed to rigid (one rigid body per bone).

The buttock region was then refined as the simulation of the body and seat interaction in the region of the buttocks and thighs is of importance for seating comfort assessment. As shown in Figure 2a, the PIPER child model coccyx appears shorter than the one of adults, likely due to the presence of growth cartilage in that region (as the coccyx is not fully ossified at 6 years old, it could not be segmented on the CT scan). As the coccyx is an important anatomical structure that is susceptible to pressure ulcer (Farshbaf et al., 2013), the coccyx was modified based on adult data. As the pelvic skeleton derived from the MRI was in a low resolution, a pelvic segmentation from an adult CT-scan that is a publicly available (subject LTE605 available on www.piper-project.org) was scaled and aligned onto the model pelvis (Figure 2b) and used as a reference to adjust for the structure of the coccyx (Figure 2c).

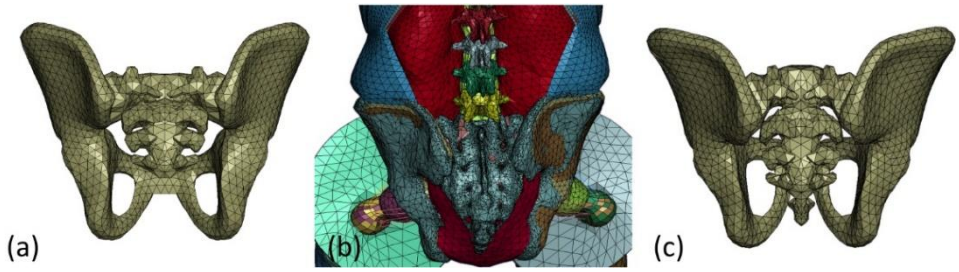

Figure 2 Extending the coccyx (a) Pelvis in the PIPER Child model (b) Aligning an adult segmentation onto the model (c) Modified pelvis with a coccyx.

Then, as depicted in Figure 3, the mesh of the soft tissue underneath the ischial tuberosity (IT) was locally refined. This area is important for seating comfort assessments since it is the place with a high risk of pressure ulcers (Tang et al., 2010) with a compressive strain of more than 50% (Elsner & Gefen, 2008; Sonenblum et al., 2013).

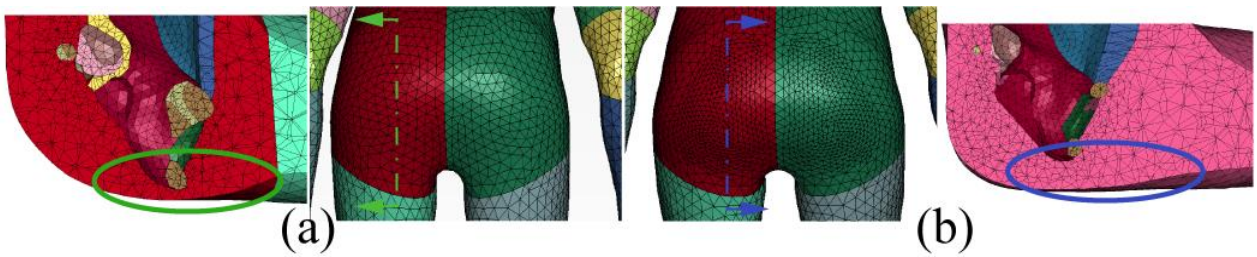

Figure 3 Local refinement of the soft tissue mesh under the ITs (a) mesh of the child model(b) refinement of the local mesh of buttocks with the adult model.

The geometry of the buttocks was obtained by the subject in a kneeling posture using a laser scan, which was not close enough to a real pre-sitting posture (Figure 4 a and b). The thickness of tissue was modified using the pre-loading seated MRI data (Wang et al., 2021). Therefore, the soft tissue-ischium initial distance was set to 40mm.

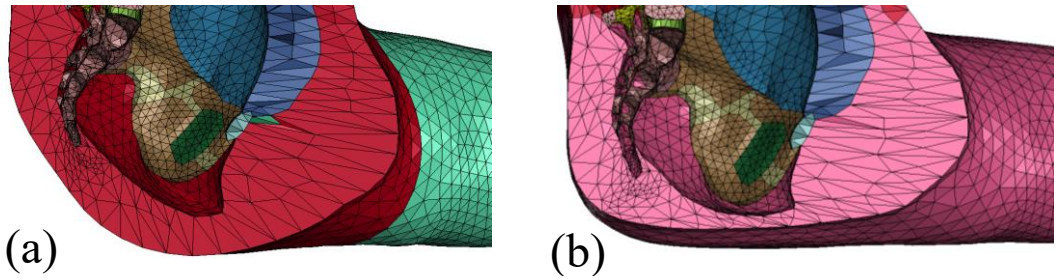

Figure 4 Buttocks shape. (a) the initial model using the kneeling posture obtained buttocks geometry. (b) pre-shaped after adaptation

The soft tissue material model and properties were changed from a simplified rubber to low modulus Neohookean model as in the work of Janak (2020) on obese modeling. The mass distribution of the model was checked and aligned with those by Huang et al. (2015) through adjusting the density of soft tissue and bone. The mass proportions are now 7.41%, 16.15%, 51.53%, 4.38% for the head, the lower limbs (thigh, calf, and foot), the torso, and the upper limbs (upper arm, forearm, and hands), respectively. Finally, some small penetrations and negative volume elements were fixed manually.

Model validation

Experiment data collection

To validate the model, an experiment was carried out with a reconfigurable experimental seat (Beurier et al., 2017). The participant was the person whose external scans and internal skeleton information were used as targets for the model development (Liu et al., 2020). Two wooden flat rectangular plates covered by a foam of 50 mm thick were used for the seat pan (620 by 565 mm) and the seat backrest (550 by 550 mm). To measure the contact pressure, two sensor mats (XSENSOR, X3 PRO V6, Canada) were attached to the foam. Four configurations were tested randomly (SPA order 0°,10°,15°,5°) while the seat pan to backrest angle (SP2BA) was fixed at 100° (Figure 5) corresponding to the seating configuration used in the MRI study by Beillas et al (2009). For each configuration, the participant was allowed to adjust the seat pan

length and the foot support height to be seated comfortably. The subject was instructed to half flex his knees and the popliteal to the frontal seat edge was about 40mm.

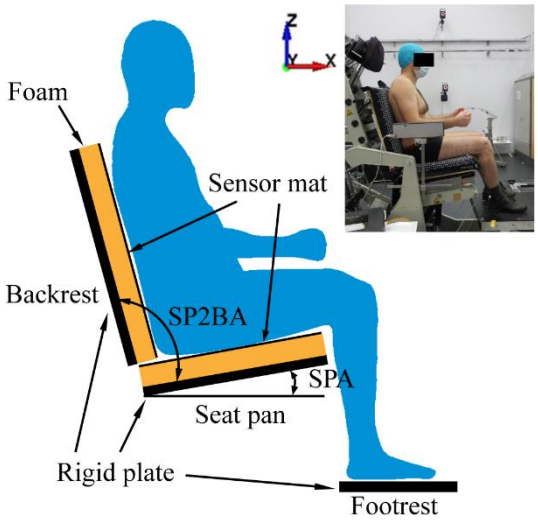

Figure 5. Experimental seat.

FE Simulation

The four experimental seating conditions were simulated with the developed adult model using LS-DYNA R11 MPP solver using 64 cores of a cluster. The time step was 2μs. Relaxation was used to help stabilize the contact force. The results (pressure, forces, etc.) were gathered at 400ms of simulation time, which took about 6 hours of elapsed time on the machines used for each simulation.

FE model prepositioning and boundary conditions

The bottom of the seat pan and backrest were fixed. The FE model was pre-positioned so that the back, buttocks and thighs were as close as possible to the seat without getting into contact. The feet were put on the footrest, which was simulated as a massless rigid body. To better control the distribution of the contact forces on the backrest, seat pan and footrest, the actual contact force on the footrest measured experimentally was imposed. For this, the footrest was oriented so that its normal direction was the same as the contact force measured experimentally. It was allowed to move only in this direction.

Automatic surface to surface contact was defined for the backrest and seat pan with a coefficient of friction (COF) of 0.1 (covered with the sensor map), while a COF of 0.4 was used for the footrest and foot contact (Derler et al., 2008). To reduce computational time and maintain posture, we constrained some bones into one rigid body so that no relative movements were allowed between them: the skull and cervical spine, the

calf and foot (left and right), the upper limb bones including the humerus, radius, ulna, hand (right and left bones). A gravity loading environment was applied.

To obtain the property of foam, strain-stress curves were obtained through compression tests with a sample size of 8×8×5 cm using an Instron material testing machine. The curves are provided in the appendix.

Data analyses

Pressure and contact seat pan force related parameters were compared between simulations and experiments. Pressure-related parameters include contact area (ContactA), mean pressure (MeanP), peak pressure (PeakP), and frontal and lateral pressure profiles (summation of pressure in rows and columns).

Results

Simulated and measured pressure distributions and profiles on the seat pan were compared in **Error! Reference source not found.** within the four-seat configurations. FE simulations were able to approach the corresponding measured pressure distributions (Figure 6a left), with some discrepancies on the thighs and between the ITs. Some left/right asymmetry was visible in the experimental data, while the model responded symmetrically as expected. The differences were more pronounced for the backrest (Figure 6a left), with some contacts near the pelvis which were not visible in the experiment. Predicted pressure profiles (Figure 6b) were close to the experimental data.

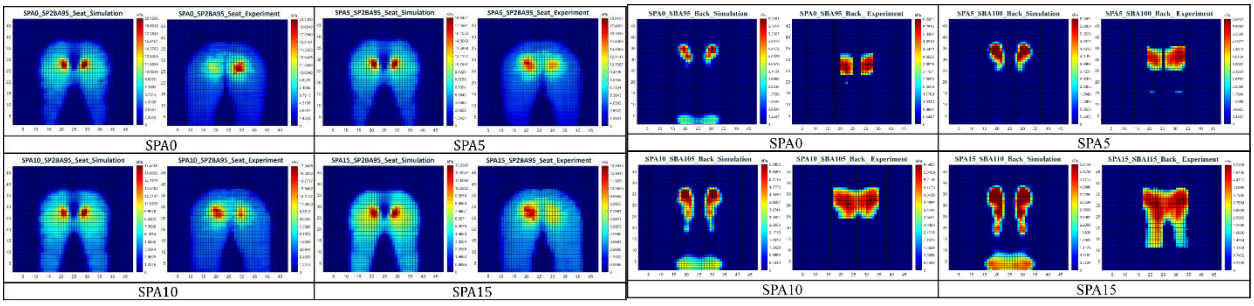

(a)

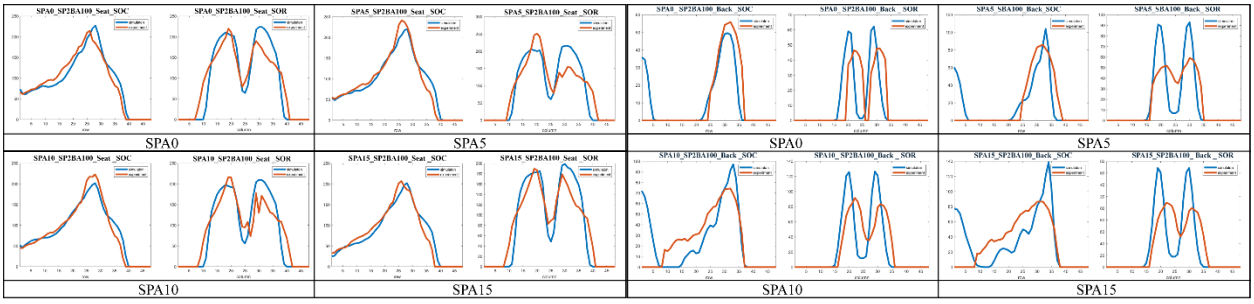

(b)

Figure 6. Simulation versus experimental pressure of four seat configurations (SPA5° to SPA15°). (a) seat (left) and backrest (right) pressure distributions are shown for the four seat configurations. (b) pressure profiles of summation of pressure in columns (SOC) and in rows (SOR). For each comparison, the simulation on the left and the experiment on the right.

The pressure, contact area, and seat forces trends for the four SPAs are summarized in Table 1. Compared to experimental data, simulation had an average error of -3.2%, 3.8% and 8.1% respectively for contact area, peak pressure and mean pressure. Concerning contact force on the seat pan, simulated shear and normal forces showed the same trend as experimental observations when increasing seat pan angle. However, a high error in percentage was observed for shear force (up to 36%).

Table 1 Simulated (S) and experimental (E) values of contact area (ContactA), peak (PeakP), and mean pressures (MeanP), and contact forces: seat pan shear force (SP_SF), and normal force (SP_NF), as well as the errors (%) of simulation relative to experiment.

SPA	ContactA (mm^2)		PeakP (kPa)			MeanP (kPa)			SP_SF(N)			SP_NF (N)		
(°)	(S)	Error	(S)	(E)	Error	(S)	(E)	Error	(S)	(E)	Error	(S)	(E)	Error
0	162257.7	-4.0	16.8	16.3	3.4	4.6	4.3	8.7	58.7	59.2	-0.5	-709.0	-697.0	-12.0
5	161128.7	-2.6	17.4	20.0	-12.9	4.5	4.3	6.4	56.1	28	28.1	-689.5	-694.3	4.8
10	159031.9	-4.8	15.2	15.1	0.8	4.4	4.0	8.5	37.7	0.6	37.1	-661.6	-652.8	-8.8
15	153225.5	-3.7	15.4	12.4	23.9	4.2	3.9	8.7	31.8	-4.2	36.0	-607.9	-597.4	-10.5
Mean	158911.0	-3.2	16.2	15.9	3.8	4.6	4.1	8.1	46.1	20.9	25.2	-667.0	-660.4	-6.6
SD	3480.6	0.8	0.9	2.7	13.2	0.1	0.2	1.0	11.55	25.3	15.2	38.0	40.4	6.7

Discussion and Conclusions

Compared to experimental observations, simulated pressure distribution showed good agreement. Although the model did not simulate muscle forces, the targeted postures correspond to a relaxed state in which the muscle forces were expected to be small. The passive stiffness of the model and the choice of initial conditions hence played a role in the response. For example, the contact in the pelvic region could be avoided if the pelvis was positioned further away from the backrest. Overall, while the choice of passive properties and boundary conditions appeared reasonable for the relaxed seating with a SP2BA of about 100°. They may need to be adjusted for postures that would further differ from the validation conditions (e.g. more reclined seating).

According to Figure 6, the backrest contacts distribution and profiles had some differences compared to the experiment, especially in the buttocks area and the location of the scapula. In simulations, the backrest size was defined according to the size of the pressure mat for comparing the pressure distributions, which was 609.6 mm in length (59.6 mm larger than the foam). Therefore, the backrest had a larger area on the buttocks than the real conditions. According to Figure 6a in right, the backrest contact peak pressures were generally

higher than in the experiment. The peak pressures were located at the two scapulas, which are covered with thin soft tissues. As described in Liu et al. (2020), the position of the scapular was palpated in a standing posture and it may be displaced when changing into a sitting posture.

Simulated shear force on the seat pan (SP_SF) showed the same trend with the experiment (Table 1) but with larger values. In the present study, the footrest contact force was imposed. It may be of interest to impose the seat pan contact force instead to better simulate the loading on the buttocks and thighs.

In this preliminary validation, only four configurations were tested with a fixed seat pan to backrest angle of 100°. Therefore, more seat configurations are needed to test the effect of seat parameters. Since the compression of the soft tissue under the ischial tuberosities was an important factor to evaluate seating comfort, the model will be further validated with soft tissue compressive deformations and observed using an open MRI (Wang et al., 2021).

In a summary, a personalized model for seating comfort was developed and its predictions in terms of force and contact pressure distribution were checked against experimental data in four postures. The models showed a reasonable agreement and further work will be conducted to expand upon the validation with more postures and the analysis of more local tissue deformation. The model will be published under an open source license to facilitate reuse.

Acknowledgments

One of authors was funded by the China Scholarship Council [grant number 202006020192].

References

Al-Dirini, R. M. A., Reed, M. P., Hu, J., & Thewlis, D. (2016). Development and Validation of a High Anatomical Fidelity FE Model for the Buttock and Thigh of a Seated Individual. *Annals of Biomedical Engineering*, *44*(9), 2805–2816. https://doi.org/10.1007/s10439-016-1560-3

Beillas, P., Giordano, C., Alvarez, V. S., Li, X., Ying, X., Kirscht, S., & Kleiven, S. (2016). Development and Performance of the PIPER Scalable Child Human Body Models. *14th International Conference Protection of Children in Cars. Dec 8-9, 2016, Munich, Germany*, 1–19.

Beillas, P., Lafon, Y., & Smith, F. W. (2009). The effects of posture and subject-to-subject variations on the position, shape and volume of abdominal and thoracic organs. *Stapp Car Crash Journal*, *53*(November), 127–154.

Beurier, G., Cardoso, M., & Wang, X. (2017). A New Multi-Adjustable Experimental Seat for Investigating Biomechanical Factors of Sitting Discomfort. *SAE Technical Paper Series*, *1*. https://doi.org/10.4271/2017-01-1393

Cheng, Z., Smith, J. A., Pellettiere, J. A., & Fleming, S. M. (2018). *Considerations and Experiences in Developing an FE Buttock Model for Seating Comfort Analysis*. *724*.

De Looze, M. P., KUIJT-EVERS, L. F. M., & VAN DIEËN, J. (2003). Sitting comfort and discomfort and the relationships with objective measures. *Ergonomics*, *46*(10), 985–997. https://doi.org/10.1080/0014013031000121977

Derler, S., Kausch, F., & Huber, R. (2008). Analysis of factors influencing the friction coefficients of shoe sole materials. Safety Science, 46(5), 822–832. https://doi.org/10.1016/j.ssci.2007.01.010

Tomas Janak, 2020. Personalization of human body models to simulate obese occupants in automotive safety, pp.140,PhD thesis.

Du, X., Ren, J., Sang, C., & Li, L. (2013). Simulation of the interaction between driver and seat. *Chinese Journal of Mechanical Engineering*, *26*(6), 1234–1242. https://doi.org/10.3901/cjme.2013.06.1234

Elsner, J. J., & Gefen, A. (2008). Is obesity a risk factor for deep tissue injury in patients with spinal cord injury? *Journal of Biomechanics*, *41*(16), 3322–3331. https://doi.org/10.1016/j.jbiomech.2008.09.036

Farshbaf, M., Yousefi, R., Pouyan, M. B., Ostadabbas, S., Nourani, M., & Pompeo, M. (2013). Detecting high-risk regions for pressure ulcer risk assessment. *Proceedings - 2013 IEEE International Conference on Bioinformatics and Biomedicine, IEEE BIBM 2013*, 255–260. https://doi.org/10.1109/BIBM.2013.6732499

Grujicic, M., Pandurangan, B., Arakere, G., Bell, W. C., He, T., & Xie, X. (2009). Seat-cushion and soft-tissue material modeling and a finite element investigation of the seating comfort for passenger-vehicle occupants. *Materials and Design*, *30*(10), 4273–4285. https://doi.org/10.1016/j.matdes.2009.04.028

Huang, S., Zhang, Z., Xu, Z., & He, Y. (2015). Modeling of human model for static pressure distribution prediction. *International Journal of Industrial Ergonomics*, *50*. https://doi.org/10.1016/j.ergon.2015.09.017

Le, P., & Marras, W. S. (2016). Evaluating the low back biomechanics of three different office

workstations: Seated, standing, and perching. *Applied Ergonomics*, *56*, 170–178. https://doi.org/10.1016/j.apergo.2016.04.001

Levy, A., Kopplin, K., & Gefen, A. (2014). An air-cell-based cushion for pressure ulcer protection remarkably reduces tissue stresses in the seated buttocks with respect to foams : Finite element studies. *Journal of Tissue Viability*, *23*(1), 13–23. https://doi.org/10.1016/j.jtv.2013.12.005

Liu, S., Beillas, P., Ding, L., & Wang, X. (2020). Morphing an Existing Open Source Human Body Model into a Personalized Model for Seating Discomfort Investigation. *SAE Technical Papers*, *2020-April*(April). https://doi.org/10.4271/2020-01-0874

Oomens, C. W. J., Bader, D. L., Loerakker, S., & Baaijens, F. (2015). Pressure Induced Deep Tissue Injury Explained. *Annals of Biomedical Engineering*, *43*(2), 297–305. https://doi.org/10.1007/s10439-014-1202-6

D. Bader. Pressure Ulcer Research Current and Future Perspectives (M), in: C. Oomens (Eds.), Springer-Verlag Berlin·Heidelberg Germany, 2005, 150-155.

Sonenblum, S. E., Sprigle, S. H., Cathcart, J. M. K., & Winder, R. J. (2013). 3-dimensional buttocks response to sitting: A case report. *Journal of Tissue Viability*, *22*(1), 12–18. https://doi.org/10.1016/j.jtv.2012.11.001

Tang, C. Y., Chan, W., & Tsui, C. P. (2010). Finite Element Analysis of Contact Pressures between Seat Cushion and Human Buttock-Thigh Tissue. *Engineering*, *02*(09), 720–726. https://doi.org/10.4236/eng.2010.29093

Wang, X., Savonnet, L., & Duprey, S. (2021). A Preliminary Study on the Effects of Foam and Seat Pan Inclination on the Deformation of the Seated Buttocks Using MRI. Lecture Notes in Networks and Systems, 223 LNNS(0), 434–438. https://doi.org/10.1007/978-3-030-74614-8_55

Yadav, S. K., Huang, C., Mo, F., Li, J., Chen, J., & Xiao, Z. (2021). Analysis of seat cushion comfort by employing a finite element buttock model as a supplement to pressure measurement. *International Journal of Industrial Ergonomics*, *86*(May 2020), 103211. https://doi.org/10.1016/j.ergon.2021.103211

Appendix

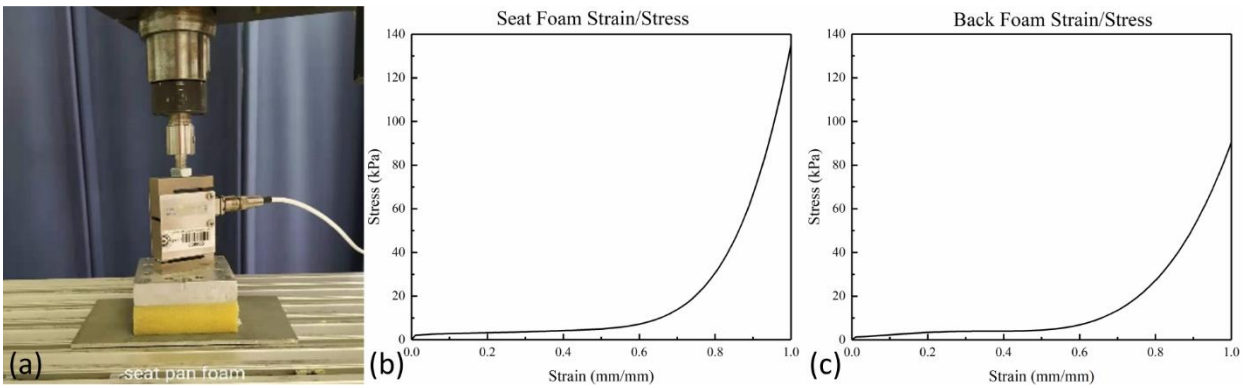

Seat pan and backrest foam strain-stress curve